

# UNLOCK PREDICTABLE SCALING FROM EMERGENT ABILITIES

Shengding Hu<sup>1</sup>, Xin Liu<sup>2</sup>, Xu Han<sup>1</sup>, Xinrong Zhang<sup>1</sup>, Chaoqun He<sup>1</sup>, Weilin Zhao<sup>1</sup>,  
Yankai Lin<sup>3</sup>, Ning Ding<sup>1</sup>, Zebin Ou<sup>4</sup>, Guoyang Zeng<sup>5</sup>, Zhiyuan Liu<sup>1\*</sup>, Maosong Sun<sup>1\*</sup>

<sup>1</sup>Department of Computer Science and Technology, Tsinghua University

<sup>2</sup>Beijing Language and Culture University.

<sup>3</sup>Renmin University of China. <sup>4</sup>Zhihu Inc. <sup>5</sup>Modelbest Inc.

hsd23@mails.tsinghua.edu.cn

## ABSTRACT

The scientific scale-up of large language models (LLMs) necessitates a comprehensive understanding of their scaling properties. However, the existing literature on the scaling properties only yields an incomplete answer: optimization loss decreases predictably as the model size increases, in line with established scaling law; yet no scaling law for task has been established and the task performances are far from predictable during scaling. Task performances typically show minor gains on small models until they improve dramatically once models exceed a size threshold, exemplifying the “emergent abilities”. In this study, we discover that small models, although they exhibit minor performance, demonstrate critical and consistent task performance improvements that are not captured by conventional evaluation strategies due to insufficient measurement resolution. To measure such improvements, we introduce PASSUNTIL, an evaluation strategy with theoretically infinite resolution, through massive sampling in the decoding phase. With PASSUNTIL, we conduct a quantitative investigation into the scaling law of task performance. The investigation contains two parts. Firstly, a strict *task scaling law* that is not conventionally known to exist, is identified, enhancing the predictability of task performances. Remarkably, we are able to predict the performance of the 2.4B model on code generation with merely 0.05% deviation before training starts, which is the first systematic attempt to verify predictable scaling proposed by GPT-4’s report (OpenAI, 2023). Secondly, underpinned by PASSUNTIL, we observe concrete evidence of emergent abilities and ascertain that they are not in conflict with the continuity of performance improvement. Their semblance to break-through is that their scaling curve cannot be fitted by standard scaling law function. We then introduce a mathematical definition for the emergent abilities. Through the definition, we refute a prevalent “multi-step reasoning hypothesis” regarding the genesis of emergent abilities and propose a new hypothesis with a satisfying fit to the observed scaling curve.

*“See the world in a grain of sand”*

## 1 INTRODUCTION

Large Language Models (LLMs) (Devlin et al., 2018; Raffel et al., 2020; Brown et al., 2020; Chowdhery et al., 2022) have become a center of interest among AI researchers recently. These models, trained on expansive datasets and furnished with an enormous number of parameters, have demonstrated unparalleled proficiency across diverse domains, such as text generation (Dubois et al., 2023), code completion (Chen et al., 2021; Rozière et al., 2023), and academic test (Hendrycks et al., 2020).

The impressive success of these LLMs depends heavily on scaling up the model parameters and pre-training data volume. It has been consistently observed that, when considering a continuum of models with nearly identical architectures, larger models coupled with increased pre-training corpora consistently yield diminished training loss. This observation has been mathematically formalized as the scaling law of loss (Kaplan et al., 2020; Henighan et al., 2020), which states that the

\*Corresponding Authors.

reducible loss achieved by the model in the log scale is linear to the model size in the log scale. Scaling law has provided guidance for the scientific scaling of LLMs, including determining the balance of the model size and pre-training data size (Hoffmann et al., 2022; Muennighoff et al., 2023). This has transformed what was once a somewhat blind scaling process into a methodology underpinned by empirical assurance. Nonetheless, such beneficial scaling law yield predictions solely on the loss, not extending to the real task performance encountered in practice. This divergence establishes a substantial gap in a comprehensive scaling-up methodology (Ganguli et al., 2022).

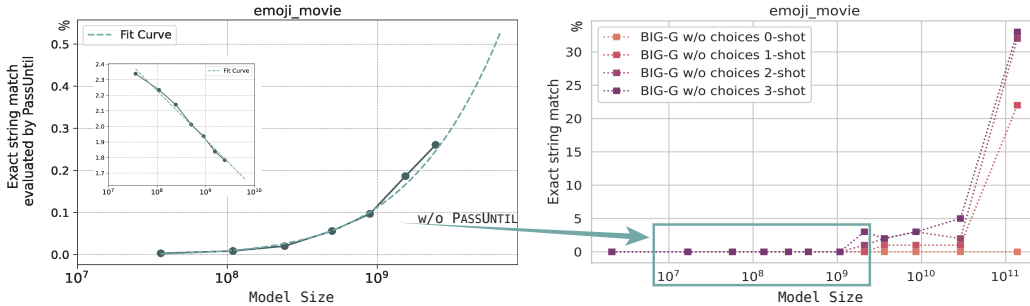


Figure 1: We can discriminate subtle performance improvement (left), which is evaluated as all zeros in conventional methods (right). The right figure directly uses Figure 9(a) in Sorscher et al. (2022) as a comparison, which the authors utilize to illustrate a “break-through” behavior in task performance. The internal figure inside the left figure shows the performances in a  $\log(-\log(\cdot))$  space, which displays strong linearity, supporting the task scaling law (Eq.(3)).

The challenge in extending loss scaling law to task performance predominantly stems from the *discontinuity* observed in task performance during scaling. Language models below a certain size yield trivial performance, i.e., random guessing on multiple choices or zero scores on generation tasks. However, when the model size surpasses a certain threshold, a distinct surge in performance appears, which leads to substantially non-trivial performance. This phenomenon is summarized as the “emergent abilities” (Srivastava et al., 2022; Wei et al., 2022a), and is observed across various model families and tasks. It seems that qualitative changes happen inside the model, which makes the model start to manifest unique capabilities. While these emerging phenomenon indicate that LLMs are becoming stronger, they complicate the prediction on task performance.

A pivotal question arises: **can we unlock predictable scaling of the task performance, from the apparent discontinuities?** We hypothesize that the perceived discontinuity from trivial to excellent performance might stem from limited evaluation resolution<sup>1</sup>. By employing a more nuanced resolution, one could potentially uncover the scaling law for tasks. Our hypothesis diverges significantly from that of Schaeffer et al. (2023), which posits that employing other continuous metrics can cause emergent abilities to disappear. A limitation of their hypothesis is that the alternative smooth metrics (e.g., distribution distance) yield insufficient insights into the target metrics (e.g., exact match) that evaluators intuitively perceive. For example, test loss is smoother than other metrics, but it does not reveal the real task performance of a code generation problem. In contrast, we target at directly predict the performance such as code generation in our experiments.

In light of this viewpoint, we introduce an evaluation strategy named PASSUNTIL that, for the first time, enables quantitative exploration of the scaling properties of task performance. PASSUNTIL deploys extensive random sampling in the decoding phase (e.g.,  $10^5$  sampling times), and evaluates each sampling result *until* any generation passes the target test. Therefore, this evaluation strategy has infinite measurement resolution as long as computational resources are not bounded. Moreover, it can provide unbiased estimates of target metrics such as accuracy and exact match. To refine our evaluation resolution and accuracy, we suggest fitting to instance-level scaling law since different test instances might have different speeds of performance improvement during scaling.

With the proposed evaluation strategy, we delve into the scaling law governing task performance. To begin with, we train two series of models ranging from 0.03B to 2.4B. These models strictly adhere to pre-training loss scaling law, providing a solid foundation for analyzing task performance scaling behavior. We mainly disclose two findings in our exploration.

<sup>1</sup>By “resolution”, we view evaluation as a measurement of the real probability of completing a task. And resolution is the smallest probability difference that the evaluation strategy can detect.

Firstly, task performances are predictable with PASSUNTIL. We validate the presence of subtle but non-negligible performance in smaller models that can be captured by PASSUNTIL. These performances are on the order of  $10^{-5}$  and exhibit steady enhancement as the model scales up. Subsequently, we derive the mathematical form of **task scaling law**, experimentally verifying an almost strict linear relationship between  $\log(-\log(\text{PU}))$  and  $\log(N)$ , where PU denotes the estimation of target metric given by PASSUNTIL and  $N$  is the number of model parameters. This relationship enables us to attain highly accurate predictions. For instance, in the code generation task, our predictions exhibit a mere 0.05% deviation from the actual values.

Secondly, emergent abilities do exist. We discover that the shape of the task scaling curve is not uniform across tasks. Several tasks manifest scaling functions that diverge from the typical task scaling law. In other words, their scaling curve is smooth and incremental but can not be fitted by the typical scaling law function. Their scaling curve of  $\log(-\log(\text{PU}))$  w.r.t.  $\log(N)$  is concave, which is akin to “super-scaling law growth”, aligning with researchers’ anticipations regarding “emergence”. Based on this observation, we provide a mathematical definition of emergence. This precise definition facilitates the exploration of hypotheses concerning the genesis of emergence. We scrutinize the popular assumption that multi-step reasoning culminates in emergence (Schaeffer et al., 2023), and propose an alternative hypothesis. This hypothesis is predicated on potential transformer circuits (Nelson et al., 2021) that are used to explain the “grokking” phenomenon (Power et al., 2022; Varma et al., 2023). It is in harmony with the observed scaling function.

Our work represents the first open-source attempt regarding the predictability of task performance. While GPT-4’s report (OpenAI, 2023) has initiated this exploration, it has not provided comprehensive details. We will open-source all checkpoints to facilitate future research in this direction.

## 2 RELATED WORK

Predicting task performance before training is an aspirational objective for the development of predictable AI systems, and a multitude of studies approach this aim from various perspectives.

**Loss Scaling Law.** Scaling phenomena have been observed across a broad spectrum of deep learning architectures. The power-law scaling behavior of loss in RNN-based models is investigated in Hestness et al. (2017). Kaplan et al. (2020) delineate the loss scaling trends for Transformer-based language models and explores the scaling behavior of optimal hyper-parameters. They formally established the following scaling law

$$L = cN^{-\alpha} + L_0, \tag{1}$$

where  $N$  is the number of non-embedding parameters of LLM,  $c, \alpha$  are positive coefficients, and  $L_0$  is the irreducible loss representing the randomness in data. This formulation has catalyzed the proliferation of LLMs. Subsequently, scaling laws are established for various domains and scenarios, including multi-modality (Henighan et al., 2020; Zhai et al., 2022), computation constraint scenario (Hoffmann et al., 2022), data engineering (Muennighoff et al., 2023; Sorscher et al., 2022), and reinforcement learning (Gao et al., 2023). Yao & Wang (2023) extend the scaling law into loss prediction by introducing hyper-parameter scaling methods. The relationship of our work with these existing literature is twofold. First, these works concentrate on training and validation loss metrics, which do not reliably predict task performance. Second, our research builds on these scaling laws and extends the mathematical form of Eq.(1) to the scaling law of task performance.

**Scaling Behavior of Task Performance.** Despite the predictable decrement in LLM loss, task performance improvements are twisted during scaling. While some tasks, predominantly those relying on memorization of knowledge, have shown progressive improvement, numerous tasks exhibit breakthrough behavior as model size increases (Srivastava et al., 2022; Wei et al., 2022a). Wei et al. (2022a) illustrate that the concept of “emergence” is also pertinent to prompting techniques such as Chain-of-Thought (Wei et al., 2022b) and In-context Learning (Brown et al., 2020), complicating the pursuit of understanding the scaling law of task performance. It appears that the law of loss scaling offers no assurance for task performance, engendering a lack of guidance in pre-training methodology. Fortunately, several studies endeavor to demystify these emergent abilities. GPT-4’s technical report (OpenAI, 2023) reports that GPT-4’s task performance can be predicted with less than 1/10000 of computation, albeit without disclosing the methodology and acknowledging that certain abilities are still beyond prediction. Subsequent research (Schaeffer et al., 2023) attributes emergence to the employment of non-smooth metrics, proposing that alternative continuous

metrics such as probabilistic distance to the ground truth answer can morph the emergence into more incremental improvements. Contrastingly, we posit that the alternative metrics could not estimate the target metrics such as exact match, which are of paramount interest to us. Rather than circumventing the target metrics, we advocate for a higher resolution in measuring these metrics to maintain the integrity and relevance of the evaluations. Our work is the first open-source attempt to quantitatively investigate the scaling behavior of task performance.

### 3 PILOT EXPERIMENTS ON INCREASING RANDOM SAMPLE NUMBERS

We initiate our exploration by visualizing the effect of improving evaluation resolution on open-sourced models. We choose four small models and evaluate them on two subsets of BigBench task (Srivastava et al., 2022): Emoji Movie and Date Understanding (see Appendix D.4.2 and D.4.3 for the subsets). We employ beam search and random sampling (with three sample times: 1, 100, and 10,000) during decoding. If any sampled answer of a test instance is evaluated as correct, then the instance is marked as “passed”. We present the number of passed instances in Table 1.

Models	Emoji Movie				Date Understanding			
	BS	RS-1	RS-100	RS-10000	BS	RS-1	RS-100	RS-10000
Pythia-410M	0/41	0/41	2/41	31/41	0/50	0/50	8/50	42/50
Pythia-1.4B	0/41	0/41	7/41	38/41	2/50	2/50	18/50	46/50
OPT-350M	0/41	0/41	4/41	33/41	1/50	0/50	4/50	37/50
OPT-1.3B	0/41	0/41	12/41	39/41	1/50	1/50	12/50	46/50

Table 1: BS denotes beam search, RS- $K$  denotes random sampling  $K$  times.  $A/B$  denotes that  $A$  instances passed among the total  $B$  instances.

We can see that even for such tasks presenting substantial difficulty to small models, most instances are passable with enough random sampling times, which will contribute to the subtle task performance improvement. Inspired by this observation, we propose our evaluation strategy that centered around improving the resolution of evaluation.

## 4 METHODS

In this section, we describe our methods to increase the resolution of evaluation, which empowers the investigation of the scaling behavior of task performance. The first is an evaluation strategy PASSUNTIL, and the second is an instance-level scaling curve fit. We also derive the task scaling law based on the loss scaling law.

### 4.1 INFINITE RESOLUTION WITH PASSUNTIL

We view task performance evaluation as the measurement of the probability of a model completing a task. Given a task instance  $s$ , suppose the probability that a model completes it is  $P(s)$ , our job is to estimate  $\mathbb{E}_s[P(s)]$ . Randomly sampling a fixed time  $K$  could estimate  $P(s)$ . However, it is hard to define the budget  $K$  that is both acceptable in computation and has enough resolution for hard samples that have small  $P(s)$ . We propose PASSUNTIL, which performs an evaluation right after an answer is generated and determines whether it is passed before we sample the next answer. We stop sampling until  $r$  (a constant) samples have passed the evaluation and record the sampling number  $K$ . We name the estimate of  $P(s)$  as the PASSUNTIL score PU, which is defined as

$$\text{PU} = \frac{r}{\mathbb{E}[K]} \quad (2)$$

Expectation means that the estimation can be more accurate with repeated experiments. Theoretically, PU has the capability to measure success rates that are infinitesimally small. The PASSUNTIL has the following properties.

**Theorem 1.** PU is an unbiased estimate for  $P(s)$ .

*Proof.* The failure time  $f = K - r$  follows the negative binomial distribution, whose expectation is  $\mathbb{E}[f] = r \frac{1-P(s)}{P(s)}$ , therefore  $\mathbb{E}[K] = \frac{r}{P(s)}$ , which gives  $\text{PU} = \frac{r}{\mathbb{E}[K]} = P(s)$ .  $\square$

**Corollary 1.1.** PU is an unbiased estimate for the target discrete metrics, such as the exact match score.

*Proof.* Take exact match score EM as an example,  $\mathbb{E}[\text{EM}] = P(s) = \text{PU}$ .  $\square$

In practice, we set  $r$  to as small as 1 or 2 considering the efficiency of evaluation. We also set the upper bound of  $K$  to a large number, such as  $10^5$ , to prevent endless sampling. Note that many instances stop before reaching this upper-bound.

**Comments.** (1) Generally, deriving  $P(s)$  directly from the prediction probability on the ground truth solution is not feasible. This is due to two primary facts: firstly, there are likely to be multiple viable solutions; secondly, even though there is only one solution, there exist multiple decoding approaches besides the optimal tokenization to decode the solution<sup>2</sup>. (2) Currently, our evaluation strategy is designed to be applicable when a random baseline achieves  $P(s) = 0$ . In the context of multiple-choice grade as the evaluation metric, evaluations tend to exhibit a biased high score relative to the true performance of the model. This discrepancy is attributed to the possibility of achieving non-zero metrics through random guesses, which can overshadow the improvements made by smaller models. The exploration of scaling law for tasks with non-zero random baselines remains a subject for future research. (3) We consider random sampling as a viable target decoding strategy due to its widespread use in LLMs. Using greedy decoding and beam search as target decoding strategies and their relationship with random sampling poses an interesting avenue for future exploration and study.

## 4.2 FROM LOSS-SCALING LAW TO TASK SCALING LAW

Then, we derive the task scaling law that PASSUNTIL will follow. We assume that the test loss of generating the next token decreases according to the scaling law of Eq.(1).

$$\text{PU} \sim \prod_{i=1}^{|y|} P(y_i | x_{1:|x|}, y_{1:i-1}) = \prod_{i=1}^{|y|} \exp(-c_i N^{-\alpha_i} - L_{0i}), \quad (3)$$

where  $x_{1:|x|}$  is the input sequence and  $y_{1:|y|}$  is the most probable sequence that decodes the correct answer (assuming its dominance compared to other sequences). Assume that the test sample is passable given a sufficiently potent LLM, then the irreducible loss for each token  $L_{0i}$  approaches 0. And assume the test loss of each token in the answer is decreasing with uniform speed when scaling (i.e.,  $a_i = a, \forall i$ ), we can derive the following function for PU on task performance:

$$\text{PU}(c, \alpha; N) \sim \exp\left(\sum_i -c_i N^{-\alpha}\right) = \exp(-cN^{-\alpha}) \quad (4)$$

The resulting mathematical model is similar to that in GPT-4 technical report (OpenAI, 2023).

## 4.3 FITTING STRATEGY

**Dataset-level Fit.** When fitting the parameters  $c, \alpha$  in PU, a dataset-level fit is plausible. For the  $j$ -th model in the scaling curve, the individual test sample’s PU is first averaged over the test set to procure  $\log(-\log(\text{PU}(N_j)))$ , followed by a linear regression to  $\log N_j$ .

**Instance-level Fit.** We notice that differences between instances lead to different scaling behaviors, which means a dataset-level fit might not be accurate when the difficulty in the test set is diverse. For example, PU on easy questions get saturated to 1 on a small model while the hard questions still receive trivial performance (see Appendix B.1 for illustration). We propose to fit an individual PASSUNTIL score (IPU) for each question and aggregate them into an estimate for the whole dataset.

$$\text{PU}(\{c_s, a_s\}; N) = \frac{1}{|S|} \sum_s \text{IPU}(c_s, a_s; N) \quad (5)$$

<sup>2</sup>For example, [4513], [717,18], and [16,17,18] all decode into string “123” in GPT-4’s tokenizer with vocab “cl100k-base”.

## 5 PREDICTABLE SCALING EXPERIMENTS

In this section, we demonstrate how the proposed framework works in practice. We first pre-train two series of language models ranging from 0.03B to 2.4B using different dataset mixtures (code-only and code-text mixture). We predict the performance of three tasks of the 2.4B model based on the performance of the rest of the models in the series.

### 5.1 SCALING CONFIGURATIONS.

**Model Configurations.** We propose to keep a consistent “shape” of the Transformers while expanding their sizes. For the  $i$ -th model in the scaling curve, we set the number of layers to be  $4i$ , the number of attention heads to be  $\lfloor \frac{i(8+i)}{4} \rfloor$ , and the dimension of head to be 64. This results in the hidden state’s dimension  $d_m$  being  $d_h n_h$ . We set the dimension of the feed-forward layer to be  $2.5d_m$ . The specific values are listed in the model configurations in Table 4 of Appendix D.1. The architecture is similar to LLaMA (Touvron et al., 2023a) (see Appendix D.1 for details).

**Pre-training Corpora.** For series 1, we use the StarCoder dataset (Li et al., 2023) as our pre-training data. For series 2, we use a mixture of StarCoder and Pile (Gao et al., 2020) dataset. Leveraging the optimal compute LLMs (Hoffmann et al., 2022), we set the maximum pre-training tokens for each model size to be the  $20N$ , where  $N$  is the number of non-embedding parameters of the model. The detailed portion within the data mixture can be seen in Appendix D.2.

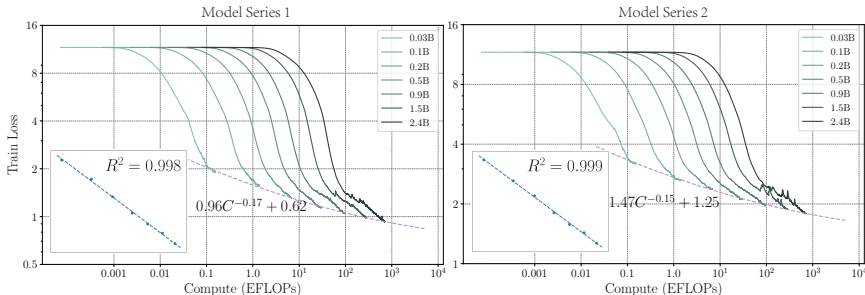


Figure 2: Training loss of the two series of models trained on different data mixtures. The internal figure illustrates the end-step reducible loss relative to model size, represented in logarithmic scale.

**Hyper-parameters.** Hyper-parameters are also of paramount importance in training a series of models that scale successfully. We examine the cosine learning rate scheduler, aligning our approach with that of Hoffmann et al. (2022), and determine the critical batch size in accordance with Kaplan et al. (2020). Nonetheless, due to constraints in space, we move the details to Appendix D.3.

### 5.2 LOSS SCALING LAW VERIFICATION.

We present the training loss curves for models in Figure 2. It is evident that the end-step training losses decrease in line with the scaling law. These empirically observed loss scaling laws lay a foundation for the subsequent approximation of task performance. Note that despite the occurrence of the loss spike in the 1.5B and 2.4B models, convergence to the scaling law is ultimately achieved, exemplifying the robustness of such an empirical law.

### 5.3 DATASET-LEVEL FIT

We select HumanEval (Chen et al., 2021), Emoji Movie, and Date Understanding (Srivastava et al., 2022) as the evaluation tasks. Note that Emoji Movie is conventionally cited as representing “emergent abilities” (Srivastava et al., 2022) (see the right figure in Figure 1). HumanEval is assessed using a zero-shot learning setting, while Emoji Movie and Date Understanding are evaluated employing 4-shot In-context Learning (Brown et al., 2020). We additionally use Chain-of-Thought Reasoning (Wei et al., 2022b) for Emoji Movie. See Appendix D.4 for the illustration and evaluation details of each task. We remove the distracting test instances from our evaluation list. For Emoji Movie, we remove the movie names that are common words (e.g., “it”) identified by NLTK (Bird

et al., 2009). These common words make the exact string match susceptible to random guess’s correctness ( See Appendix D.5 for details).

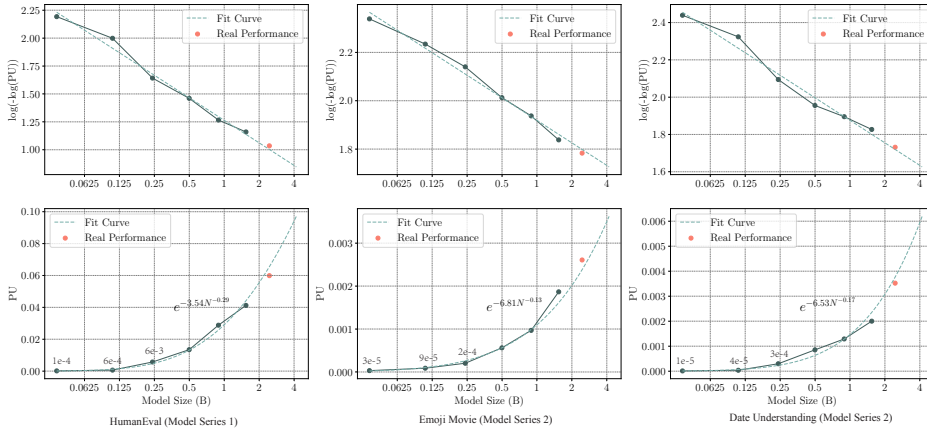


Figure 3: Task performance scales predictably with model scale. The red points denote the real performance of 2.4B model, which are close to the task scaling laws fitted from 0.03B to 1.5B. We observe that all three tasks exhibit a strong linear relationship between  $\log(-\log(\text{PU}))$  and  $\log(N)$ , verifying the success of task scaling law given by Eq.(3). The estimation of the scaling law functions utilizes the 0.03b to 1.5B models, which predicts the performance of the 2.4B model with small yet acceptable deviations.

#### 5.4 INSTANCE-LEVEL FIT

According to § 4.3, we take the difference among test samples into consideration to improve the estimation. We plot how instance-level PASSUNTIL scales in Figure 12 of Appendix E.4. The fitted instance-level scaling laws demonstrate that the performances of different instances not only originate from unique starting points but also scale at varying rates. Nevertheless, they can be fitted by task scaling law individually. Some instances deviate from the scaling law noticeably, which needs future investigation.

Method	HumanEval (1)	HumanEval (2)	Date Understanding (2)	Emoji Movie (2)
Real Value	0.05990	0.04279	0.00346	0.002608
Dataset-level Fit	0.06550	0.05191	0.00377	<b>0.002381</b>
Instance-level Fit	<b>0.05987</b>	<b>0.04402</b>	<b>0.00352</b>	0.003112

Table 2: Prediction of our framework compared to the real performance on two series of models. The number after the task denotes the model series used in the evaluation.

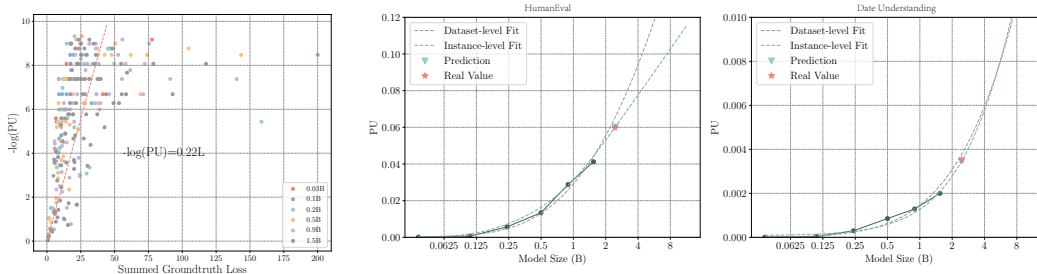


Figure 4: PU w.r.t. the test loss on HumanEval of model series 1. Figure 5: We successfully predicted the performance of 2.4B model with 0.05% deviation (left) and 1.7% deviation (right).

**Estimating PASSUNTIL from Test Loss.** Estimating at the instance level presents challenges for hard instances that lack adequate non-zero PU values for fitting. These samples may also contribute to PU as the model size increases. We suggest leveraging test loss on ground truth answers to assist the prediction for such instances. We leverage the “easy” instances, which have both test loss and non-zero PU to estimate the relation between test loss and PU (Figure 4). Then we predict the test loss of each instance on 2.4B model based on 0.03B ~ 1.5B models. Finally, we transform the predicted test loss to predicted PU according to the aforementioned relationship. Details are

presented in Appendix E.2. We provide the final prediction result of 2.4B model in Table 2, and draw the predicted PU curve in Figure 5. We can see that the predictions are accurate, with only 0.05% difference on HumanEval of series 1 and 1.7% difference on Date Understanding of series 2.

## 6 EMERGENT ABILITIES

Building on the discovery of the predictability of task performance, we proceed with our investigation into the scaling behavior emergent abilities. We prove that even with the refined resolution brought by PASSUNTIL, emergent abilities still exist with concrete evidence. We establish their mathematical definitions. Additionally, we scrutinize the “multi-step reasoning” hypothesis regarding the genesis of emergent abilities, and subsequently propose an alternative “circuit competition” hypothesis that explains our experiments.

We study the scaling curve on four subtasks in the “Unnatural In-context Learning” categories in BigBench (Srivastava et al., 2022). “Unnatural In-context Learning” is a set of tasks designed to specifically study the in-context learning ability. These tasks involve input-output pairs that have been intentionally altered to deviate from the typical training distribution, thereby necessitating the model’s focus on unconventional in-context patterns. Task details and examples are in Appendix D.4.4. We randomly select 20 questions in the test set from each task and sample 4-shot examples from the remaining questions to serve as in-context examples. The evaluation metric employed is the exact match, and the upper bound sampling time is set to  $10^5$ . When fitting the scaling curve, we only utilize the dataset-level PASSUNTIL since these test instances are manually constructed to test one skill of LLM and thus might be devoid of difficulty variation.

**Emergence Still Exists But Becomes Continuous.** The evaluation on task “Dates” and “Identity” is shown in Figure 6. Other tasks are shown in Appendix E.3. “Dates” exhibit very smooth and consistent improvement starting from 0.03B, while the other tasks are a bit twisty. Nevertheless, these in-context learning tasks all display a strictly concave function between  $\log(-\log(\text{PU}))$  and  $\log N$ , deviating from the scaling law (Eq.(3)) which requires this function to be linear. This means, unlike those tasks governed by the task scaling law, where “growth speed”  $\alpha$  is uniform across different model sizes, **there exist some tasks that see an increase in “growth speed”  $\alpha$  as models enlarge. This phenomenon echoes the “emergence” observed in previous studies.**

**Mathematical Definition of Emergence.** Now, we try to provide a mathematical definition of emergence. Since the loss scaling law of Eq.(1) is the only widely accepted principle during model scaling, we rely on its derived task scaling law of Eq.(3) as a separator between emergence and other scaling behavior.

**Definition 1.** Given a spectrum of models, we let the number of non-embedding parameters be variable  $N$ , suppose the  $\text{PU}(N)$  estimated by PASSUNTIL on a task is a continuous function of  $N$ .

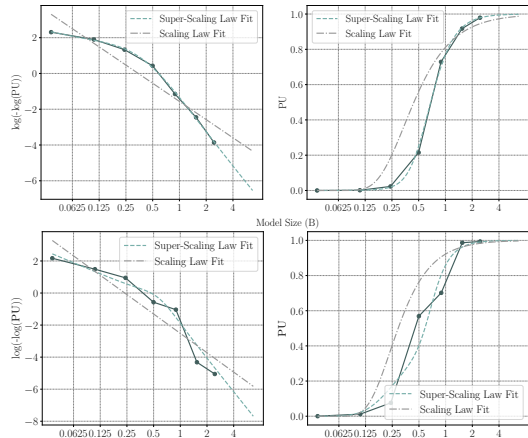


Figure 6: Scaling curve for task “Dates” and “Identity”. Concave functions are observed between  $\log(-\log(\text{PU}))$  and  $\log N$ . Scaling law fit curves are in grey and super-scaling law fit curves are in green.

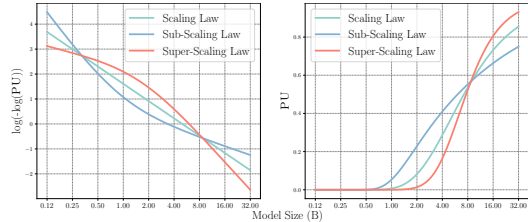


Figure 7: Three basic types of scaling curve, corresponding to convex, linear, and concave function between  $\log(-\log(\text{PU}))$  and  $\log N$ .



Define  $F(N) = \log(-\log(\text{PU}(N)))$ , then the scaling curve of a task can be categorized into three main categories:

1. if  $F(N)$  is a linear function of  $\log N$ , then the task obeys scaling law growth.
2. if  $F(N)$  is a convex function of  $\log N$ , then the task obeys sub-scaling law growth.
3. if  $F(N)$  is a concave function of  $\log N$ , then the task obeys super-scaling law growth, which can be defined as a task requires “emergent abilities”.

Figure 7 shows visualizations of three types of growth. The scaling curve of PU shows that all three types appear analogous to exponential growth when performance starts to become noticeable. However, the three types of scaling behavior are qualitatively different. Task scaling curves with task scaling law growth or sub-scaling law growth are easier to predict, whereas a super-scaling law growth is not easy to predict, which might go out of control when the model gets larger.

**The Cause of Emergence?** The above mathematical definition provides us the opportunity to examine the hypothesis regarding the genesis of emergence. Here, we study the following hypothesis:

Emergent abilities may be induced by multi-step reasoning (Srivastava et al., 2022; Wei et al., 2022a; Schaeffer et al., 2023)

We prove that, surprisingly, this hypothesis leads to sub-scaling law growth instead of emergence.

**Theorem 2.** *Suppose each reasoning step’s success rate, measured by PASSUNTIL obeys the scaling law growth, then the multi-step success rate follows the sub-scaling law growth.*

*Proof.* Suppose the success rate of reasoning step  $i$  obeys a scaling law growth with coefficient  $c_i$  and  $\alpha_i$ , then  $F(N) = \log(\sum_i c_i \exp(-\alpha_i \log N))$ . Using Cauchy–Schwarz inequality, we can prove that  $\frac{\partial^2 F}{\partial(\log N)^2} \geq 0$ . Therefore, the scaling curve is convex. See Appendix C.1 for a more elaborated proof.  $\square$

This proof can also be understood more intuitively: the growth speed will initially be boosted by the improvement of those easy steps, and eventually be bounded by the most difficult steps, thus showing a decreasing growth speed. Then, we propose an alternative hypothesis: suggesting that multiple neural “circuits” (Nelson et al., 2021) may be represented within the LLMs, and that as long as one such circuit can successfully solve the test instance, the test instance is deemed passed. This hypothesis is inspired by the explanation of “grokking” phenomenon given by Varma et al. (2023). They propose that there exists a memorization circuit and a generalization circuit inside the transformers, and the “grokking” phenomenon is led by the generalization circuit getting more efficient than the memorization circuit during training. We will demonstrate that with this hypothesis, the scaling curve exhibits characteristics of emergence.

**Theorem 3.** *Suppose multiple circuits  $i$  exist in the LLMs that are responsible for solving the task, and each displays scaling law growth and has  $\text{PU}_i$ . In this scenario, the success rate of the task is the majority voting of these circuits, i.e.,  $F(N) = \log(-\log \max_i \text{PU}_i)$ . Then,  $F(N)$  is a concave function of  $\log N$ .*

*Proof.*  $F(N) = \min_i(\log c_i - \alpha_i \log N)$ . Since the minimum operator keeps concavity,  $F(N)$  is a concave function of  $\log N$ . See Appendix C.1 for a more elaborated proof.  $\square$

We loosely test the hypothesis by fitting the scaling curve for the unnatural in-context learning task. In practice, similar to Varma et al. (2023), we adopt a soft version of the majority voting. We apply a weighted combination between two circuits. And we assume the number of the circuits is 2. Therefore, we fit  $w_1(\alpha_1 \log N - \log c_1) + w_2(\alpha_2 \log N - \log c_2)$  to  $F(N)$ , where  $w_1$  and  $w_2$  is given by the Softmax of  $\alpha_i \log N - \log c_i$ . The resulting fit curve is demonstrated in the green line in Figure 6 and Appendix E.3. We can see that this hypothesis produces fit curves that align more accurately with the observed performance scaling curve.

## 7 CONCLUSION.

Our work introduces a novel evaluation strategy capable of detecting minimal performance improvements during model scaling, thus opening avenues for quantitatively measuring the task scaling laws. This method has enabled the successful prediction of the performance of larger models. Additionally, we have performed a quantitative analysis of emergent abilities, providing a clearer insight into their nature and origination, refuting prevailing hypotheses and proposing our hypothesis. This research not only enhances our understanding of LLMs’ scaling properties but also sets the stage for future explorations in scientific scale-up of LLMs.

## ETHICAL STATEMENT

In this paper, we demonstrate that emergent abilities do exist with concrete evidence. The hypothesis regarding the cause of emergence implies that we need a better understanding of the working mechanism to produce accurate predictions for such emergent ability. Without an understanding of the working mechanism, any fit curve to the early stage of task performance improvement might be governed by another stronger, yet unknown, “generalization” circuit when the model gets sufficiently large. Thus, this hypothesis calls for deeper research into the mechanism of LLMs to prevent the safety concerns brought by emergent abilities.

## REPRODUCIBILITY STATEMENT


We will open-source all the checkpoints, and all evaluation scripts for reproducibility.

## REFERENCES

- Steven Bird, Ewan Klein, and Edward Loper. Natural language processing with Python: analyzing text with the natural language toolkit. ” O’Reilly Media, Inc.”, 2009.
- Tom Brown, Benjamin Mann, Nick Ryder, Melanie Subbiah, Jared D Kaplan, Prafulla Dhariwal, Arvind Neelakantan, Pranav Shyam, Girish Sastry, Amanda Askell, et al. Language models are few-shot learners. Advances in neural information processing systems, 33:1877–1901, 2020.
- Mark Chen, Jerry Tworek, Heewoo Jun, Qiming Yuan, Henrique Ponde de Oliveira Pinto, Jared Kaplan, Harri Edwards, Yuri Burda, Nicholas Joseph, Greg Brockman, et al. Evaluating large language models trained on code. arXiv preprint arXiv:2107.03374, 2021.
- Aakanksha Chowdhery, Sharan Narang, Jacob Devlin, Maarten Bosma, Gaurav Mishra, Adam Roberts, Paul Barham, Hyung Won Chung, Charles Sutton, Sebastian Gehrmann, et al. Palm: Scaling language modeling with pathways. arXiv preprint arXiv:2204.02311, 2022.
- Jacob Devlin, Ming-Wei Chang, Kenton Lee, and Kristina Toutanova. Bert: Pre-training of deep bidirectional transformers for language understanding. arXiv preprint arXiv:1810.04805, 2018.
- Yann Dubois, Xuechen Li, Rohan Taori, Tianyi Zhang, Ishaan Gulrajani, Jimmy Ba, Carlos Guestrin, Percy Liang, and Tatsunori B Hashimoto. AlpacaFarm: A simulation framework for methods that learn from human feedback. arXiv preprint arXiv:2305.14387, 2023.
- Deep Ganguli, Danny Hernandez, Liane Lovitt, Amanda Askell, Yuntao Bai, Anna Chen, Tom Conerly, Nova Dassarma, Dawn Drain, Nelson Elhage, et al. Predictability and surprise in large generative models. In Proceedings of the 2022 ACM Conference on Fairness, Accountability, and Transparency, pp. 1747–1764, 2022.
- Leo Gao, Stella Biderman, Sid Black, Laurence Golding, Travis Hoppe, Charles Foster, Jason Phang, Horace He, Anish Thite, Noa Nabeshima, et al. The pile: An 800gb dataset of diverse text for language modeling. arXiv preprint arXiv:2101.00027, 2020.
- Leo Gao, John Schulman, and Jacob Hilton. Scaling laws for reward model overoptimization. In International Conference on Machine Learning, pp. 10835–10866. PMLR, 2023.

- Dan Hendrycks and Kevin Gimpel. Gaussian error linear units (gelus). [arXiv preprint arXiv:1606.08415](#), 2016.
- Dan Hendrycks, Collin Burns, Steven Basart, Andy Zou, Mantas Mazeika, Dawn Song, and Jacob Steinhardt. Measuring massive multitask language understanding. [arXiv preprint arXiv:2009.03300](#), 2020.
- Tom Henighan, Jared Kaplan, Mor Katz, Mark Chen, Christopher Hesse, Jacob Jackson, Heewoo Jun, Tom B Brown, Prafulla Dhariwal, Scott Gray, et al. Scaling laws for autoregressive generative modeling. [arXiv preprint arXiv:2010.14701](#), 2020.
- Joel Hestness, Sharan Narang, Newsha Ardalani, Gregory Diamos, Heewoo Jun, Hassan Kianinejad, Md Mostofa Ali Patwary, Yang Yang, and Yanqi Zhou. Deep learning scaling is predictable, empirically. [arXiv preprint arXiv:1712.00409](#), 2017.
- Jordan Hoffmann, Sebastian Borgeaud, Arthur Mensch, Elena Buchatskaya, Trevor Cai, Eliza Rutherford, Diego de Las Casas, Lisa Anne Hendricks, Johannes Welbl, Aidan Clark, et al. Training compute-optimal large language models. [arXiv preprint arXiv:2203.15556](#), 2022.
- Jared Kaplan, Sam McCandlish, Tom Henighan, Tom B Brown, Benjamin Chess, Rewon Child, Scott Gray, Alec Radford, Jeffrey Wu, and Dario Amodei. Scaling laws for neural language models. [arXiv preprint arXiv:2001.08361](#), 2020.
- Raymond Li, Loubna Ben Allal, Yangtian Zi, Niklas Muennighoff, Denis Kocetkov, Chenghao Mou, Marc Marone, Christopher Akiki, Jia Li, Jenny Chim, et al. Starcoder: may the source be with you! [arXiv preprint arXiv:2305.06161](#), 2023.
- Niklas Muennighoff, Alexander M Rush, Boaz Barak, Teven Le Scao, Aleksandra Piktus, Nouamane Tazi, Sampo Pyysalo, Thomas Wolf, and Colin Raffel. Scaling data-constrained language models. [arXiv preprint arXiv:2305.16264](#), 2023.
- Elhage Nelson, Nanda Neel, Olsson Catherine, Henighan Tom, Joseph Nicholas, Mann Ben, Askell Amanda, Bai Yuntao, Chen Anna, Conerly Tom, DasSarma Nova, Drain Dawn, Ganguli Deep, Hatfield-Dodds Zac, Hernandez Danny, Jones Andy, Kernion Jackson, Lovitt Liane, Ndousse Kamal, Amodei Dario, Brown Tom, Clark Jack, Kaplan Jared, McCandlish Sam, and Olah Chris. A mathematical framework for Transformer circuits. 2021. URL <https://transformer-circuits.pub/2021/framework/index.html>.
- OpenAI. Gpt-4 technical report, 2023.
- Alethea Power, Yuri Burda, Harri Edwards, Igor Babuschkin, and Vedant Misra. Grokking: Generalization beyond overfitting on small algorithmic datasets. [arXiv preprint arXiv:2201.02177](#), 2022.
- Colin Raffel, Noam Shazeer, Adam Roberts, Katherine Lee, Sharan Narang, Michael Matena, Yanqi Zhou, Wei Li, and Peter J Liu. Exploring the limits of transfer learning with a unified text-to-text transformer. [The Journal of Machine Learning Research](#), 21(1):5485–5551, 2020.
- Baptiste Rozière, Jonas Gehring, Fabian Gloeckle, Sten Sootla, Itai Gat, Xiaoqing Ellen Tan, Yossi Adi, Jingyu Liu, Tal Remez, Jérémy Rapin, et al. Code llama: Open foundation models for code. [arXiv preprint arXiv:2308.12950](#), 2023.
- Rylan Schaeffer, Brando Miranda, and Sanmi Koyejo. Are emergent abilities of large language models a mirage? [arXiv preprint arXiv:2304.15004](#), 2023.
- Noam Shazeer. GLU variants improve transformer. [CoRR](#), abs/2002.05202, 2020. URL <https://arxiv.org/abs/2002.05202>.
- Ben Sorscher, Robert Geirhos, Shashank Shekhar, Surya Ganguli, and Ari Morcos. Beyond neural scaling laws: beating power law scaling via data pruning. [Advances in Neural Information Processing Systems](#), 35:19523–19536, 2022.

- Aarohi Srivastava, Abhinav Rastogi, Abhishek Rao, Abu Awal Md Shoeb, Abubakar Abid, Adam Fisch, Adam R Brown, Adam Santoro, Aditya Gupta, Adrià Garriga-Alonso, et al. Beyond the imitation game: Quantifying and extrapolating the capabilities of language models. [arXiv preprint arXiv:2206.04615](#), 2022.
- Hugo Touvron, Thibaut Lavril, Gautier Izacard, Xavier Martinet, Marie-Anne Lachaux, Timothée Lacroix, Baptiste Rozière, Naman Goyal, Eric Hambro, Faisal Azhar, et al. Llama: Open and efficient foundation language models. [arXiv preprint arXiv:2302.13971](#), 2023a.
- Hugo Touvron, Louis Martin, Kevin Stone, Peter Albert, Amjad Almahairi, Yasmine Babaei, Nikolay Bashlykov, Soumya Batra, Prajjwal Bhargava, Shruti Bhosale, et al. Llama 2: Open foundation and fine-tuned chat models. [arXiv preprint arXiv:2307.09288](#), 2023b.
- Vikrant Varma, Rohin Shah, Zachary Kenton, János Kramár, and Ramana Kumar. Explaining grokking through circuit efficiency. [arXiv preprint arXiv:2309.02390](#), 2023.
- Jason Wei, Yi Tay, Rishi Bommasani, Colin Raffel, Barret Zoph, Sebastian Borgeaud, Dani Yogatama, Maarten Bosma, Denny Zhou, Donald Metzler, et al. Emergent abilities of large language models. [arXiv preprint arXiv:2206.07682](#), 2022a.
- Jason Wei, Xuezhi Wang, Dale Schuurmans, Maarten Bosma, Fei Xia, Ed Chi, Quoc V Le, Denny Zhou, et al. Chain-of-thought prompting elicits reasoning in large language models. [Advances in Neural Information Processing Systems](#), 35:24824–24837, 2022b.
- Greg Yang, Edward J Hu, Igor Babuschkin, Szymon Sidor, Xiaodong Liu, David Farhi, Nick Ryder, Jakub Pachocki, Weizhu Chen, and Jianfeng Gao. Tensor programs v: Tuning large neural networks via zero-shot hyperparameter transfer. [arXiv preprint arXiv:2203.03466](#), 2022.
- Yiqun Yao and Yequan Wang. Research without re-search: Maximal update parametrization yields accurate loss prediction across scales. [arXiv preprint arXiv:2304.06875](#), 2023.
- Xiaohua Zhai, Alexander Kolesnikov, Neil Houlsby, and Lucas Beyer. Scaling vision transformers. In [Proceedings of the IEEE/CVF Conference on Computer Vision and Pattern Recognition](#), pp. 12104–12113, 2022.

**Note:** clicking each  in the appendix will allow you to jump back to the corresponding position in the main paper to continue reading.

## A LIMITATIONS


Our work has several limitations.

1. Firstly, we currently do not extend the prediction of task performance to much larger models (e.g., 10B and more). We will try to scale up the experiment in the future.
2. Secondly, we are not claiming that we can accurately predict the task performance on all tasks. For example, we only *fit* the scaling curve for the tasks that display emergence. We still have a long way to go before we can *predict* these tasks. Even for the tasks that might not display “emergence”, we currently do not complete a thorough prediction for them. We will add predictions on more of these tasks in the future. That said, predictable scaling, as OpenAI points out (OpenAI, 2023), is still a very challenging and aspirational goal for AI researchers. Our work serves as the initial attempt to it.
3. Thirdly, although we propose a hypothesis regarding the cause of emergent abilities, our validation for the hypothesis is superficial. We satisfactorily fit the scaling curve under this hypothesis. However, whether this hypothesis is true from the underlying mechanism remains unknown.

## B SUPPLEMENTARY MATERIALS FOR PASSUNTIL

In this section, we provide some additional comments about our evaluation strategy. We present our intuition for instance-level PASSUNTIL.

### B.1 INSTANCE-LEVEL PASSUNTIL INTUITION.


 Table 3 delineates the PASSUNTIL for both an easy and a challenging instance within HumanEval. It was observed that with an increase in model size, the easier instance (index 24) exhibited a higher PU. However, the more challenging instance (index 20) continued to manifest trivial performance, suggesting a potential variance in their respective scaling curves. Blindly averaging performance over instances will make the improvement on hard instances vanish compared to the easy ones, leading to an inaccurate prediction after the model gets saturated in the easy instances.

Instance index	PASSUNTIL					
	0.03B	0.1B	0.2B	0.5B	0.9B	1.5B
20	0	0	0	0.000625	0.001875	0.008125
24	0.00375	0.05125	0.350625	0.3625	0.568125	0.796875

Table 3: In HumanEval, an easy instance (index 24) gets a much higher PU compared to the hard one (index 20).

## C SUPPLEMENTARY MATERIALS ON EMERGENT ABILITIES

### C.1 THEORETICAL ANALYSIS OF HYPOTHESIS

 We present the proof of two theorems about the cause of emergent abilities in Section 6 briefly. In this section, we provide the elaborated proofs.

**Theorem 2.** *Suppose the success rate of each reasoning step  $i$ , measured by PASSUNTIL, obeys the scaling law growth. Then the multi-step’s success rate follows the sub-scaling law growth.*

*Proof.* Suppose the PU of reasoning step  $i$  obeys a scaling law growth with coefficient  $c_i$  and  $\alpha_i$ , The overall success rate is

$$\begin{aligned} F(N) &= \log \left( -\log \prod_i P_i \right) \\ &= \log \left( -\log \prod_i \exp(-c_i \exp(-\alpha_i \log N)) \right) \\ &= \log \left( \sum_i c_i \exp(-\alpha_i \log N) \right) \end{aligned} \quad (6)$$

Then we take the second derivative of the  $F(N)$  over  $\log N$ , we can get

$$\begin{aligned} \frac{\partial^2 F}{\partial(\log N)^2} &= \frac{\sum_i \alpha_i^2 c_i \exp(-\alpha_i \log N) \sum_i c_i \exp(-\alpha_i \log N)}{(\sum_i c_i \exp(-\alpha_i \log N))^2} \\ &\quad - \frac{(\sum_i \alpha_i c_i \exp(-\alpha_i \log N))^2}{(\sum_i c_i \exp(-\alpha_i \log N))^2} \end{aligned} \quad (7)$$

Let  $k_i = c_i \exp(-\alpha_i \log N) > 0$ , the Eq.(7) is

$$\frac{\sum_i \alpha_i^2 k_i \sum_i k_i - (\sum_i \alpha_i k_i)^2}{(\sum_i k_i)^2} \quad (8)$$

Using Cauchy–Schwarz inequality, we can prove that

$$\frac{\partial^2 F}{\partial(\log N)^2} \geq 0, \quad \forall \alpha_i > 0, c_i > 0 \quad (9)$$

Only when  $\alpha_i \sqrt{k_i} / \sqrt{k_i} = \text{Constant}$ , the equation holds, i.e., when all the steps in the reasoning chain scale with the same speed. Thus,  $F(N)$  is a convex function of  $\log N$ , and the scaling curve exhibits sub-scaling law growth.  $\square$

**Theorem 3.** *Suppose multiple circuits exist in the LLMs that are responsible for solving the task, each displays scaling law growth, the PASSUNTIL of the task is the majority voting of these circuits, i.e.,  $F(N) = \log(-\log \max_i P_i)$  Then,  $F(N)$  is a concave function of  $\log N$ .*

*Proof.*


$$\begin{aligned} F(N) &= \log \left( -\log \max_i \exp(-c_i \exp(-\alpha_i \log N)) \right) \\ &= \log \min_i c_i \exp(-\alpha_i \log N) \\ &= \min_i (\log c_i - \alpha_i \log N) \end{aligned} \quad (10)$$

Since the minimum operator keeps concavity,  $F(N)$  is a concave function of  $\log N$ .  $\square$

## D DETAILS OF EXPERIMENTAL CONFIGURATIONS

In this section, we detail the model configurations, training configurations, and data mixtures used for the two series of models.


### D.1 MODEL CONFIGURATION

 Table 4 shows the detailed model configurations and training configuration of the series models in the scaling curve, which aims to keep a uniform “shape” while expanding the model size. We use a similar architecture to Llama 2 (Touvron et al., 2023b). Some minimal differences include: we use tied embedding between the input and output embeddings, and we use gated-GeLU (Hendrycks & Gimpel, 2016) instead of gated-SiLU (Shazeer, 2020).


Name	i	N (B)	$d_m$	$d_{ff}$	$d_h$	$n_h$	$L$	BS (M)	TS	Tokens (B)
\	i	\	$d_h n_h$	$2.5d_m$	64	$\lfloor \frac{i(8+i)}{4} \rfloor$	$\lfloor 4i \rfloor$	\	\	\
0.03B	3	0.036	512	1280	64	8	12	0.33	2196	0.72
0.1B	4	0.109	768	1920	64	12	16	0.88	2464	2.18
0.2B	5	0.241	1024	2560	64	16	20	1.57	3064	4.82
0.5B	6	0.499	1344	3360	64	21	24	2.10	4758	9.99
0.9B	7	0.892	1664	4160	64	26	28	2.95	6049	17.9
1.5B	8	1.542	2048	5120	64	32	32	4.26	7230	30.8
2.4B	9	2.45	2432	6080	64	38	36	5.51	8900	49.0

Table 4: Model configurations and training configurations of the models in the scaling curve. N(B) represents the number of non-embedding parameters of the model, measured in billions. BS(M) indicates the number of tokens in a batch (i.e., batch size) used to train the model, measured in millions. TS denotes the training steps. Tokens(B) refers the total number of tokens used to train the model.

## D.2 PRE-TRAINING CORPORA

 We pre-train two series of LLMs using different data mixtures to demonstrate the generality of our experiments. Tables 5 and 6 respectively display the specific data mixture proportions for Series 1 and Series 2 LLMs.

## D.3 HYPER-PARAMETERS STUDY

 **Learning Rate.** We use a cosine learning rate scheduler, analogous to those in preceding studies (Touvron et al., 2023a;b; Hoffmann et al., 2022). The maximum learning rate is consistently fixed at 0.01 across varying model scales, with no significant loss explosion at this rate. This stability is potentially attributed to our normalization strategies (Yang et al., 2022) and increased batch size across scales. Echoing findings from Hoffmann et al. (2022), we ascertain that for training LLMs up to a specific end step, the optimal cycle length of the cosine learning rate scheduler is equivalent to the end step. Deviations from this optimal cycle length, either longer or shorter, result in sub-optimal performance.

**Batch Size.** To estimate the optimal batch size required for model pre-training, we replicate the experiments in alignment with Kaplan et al. (2020) to determine the optimal batch size of a model and adjust the real batch size slightly from the optimal batch size to maximize GPU utility. The values of batch sizes and train steps are listed in Table 4.


Corpora	Token Portion
StarCoder_Python	0.3
StarCoder_Others	0.7

Table 5: Pre-training corpora used for scaling the Code LLMs (model series 1).

Corpora	Token Portion
StarCoder_Python	0.15
StarCoder_Others	0.12
Stack_Overflow	0.03
Arxiv	0.05
Pile	0.65

Table 6: Pre-training corpora used for scaling the Code-Text LLMs (model series 2).

## D.4 TEST SET CONFIGURATIONS

 In this section, we introduce the test sets and evaluation details in our experiments.

### D.4.1 HUMAN EVAL

The HumanEval (Chen et al., 2021) dataset released by OpenAI encompasses 164 programming problems. Each problem is composed of a function signature, a docstring, a body, and multiple unit tests. Our assessment of this dataset is conducted utilizing a zero-shot approach. The completion of

code, as generated by LLMs, is deemed passed only if it successfully passes all unit tests. For our evaluations, we set the upper bound of sampling times in PASSUNTIL to  $10^4$ .

#### D.4.2 EMOJI MOVIE

👉 Emoji Movie is a subtask of BigBench (Srivastava et al., 2022) and requires LLMs to identify well-known movies from their plots described using emojis. Our evaluation methodology incorporates the use of Chain-of-Thought (CoT) and 4-shot In-context Learning. We randomly select 41 test instances (initially 50 instances, with 9 distracting instances removed, see Appendix D.5) to constitute our test set and arbitrarily designate 4 instances as few-shot contexts. For CoT, we use GPT-4 to generate prompts for each instance in the few-shot context. The model is expected to read the 4-shot in-context examples, generate a thought, and then provide the answer. Our evaluation methodology employs extract string match, i.e. where the output of the model contains the target film name. We set the sampling upper bound times set to be  $10^5$ .

#### D.4.3 DATE UNDERSTANDING

👉 Date Understanding, a subset of BigBench (Srivastava et al., 2022), is constructed to evaluate the capability of LLMs in comprehending dates, by posing questions related to the date reasoning. For the evaluation of this task, we employ a 4-shot In-context Learning. We randomly sample 47 instances to form the test set (initially 50 instances, with 3 distracting instances removed, see Appendix D.5). We random sample 4 instances from the remaining dataset to serve as in-context examples. We also use extract string match to measure the output from LLMs and set the sampling upper bound times to  $10^5$ .

#### D.4.4 UNNATURAL IN-CONTEXT LEARNING TASKS

👉 The Unnatural In-context Learning tasks serve as a series of distinctive subtasks within BigBench (Srivastava et al., 2022). These subtasks are designed to assess the models’ ability to perform in-context learning where the context sequences are intentionally altered to be likely outside of the training distribution, necessitating the model’s attention to unconventional in-context patterns. Some instances of these subtasks are exemplified in Table 7. For each task, 20 instances are randomly sampled to compose the test set, utilizing a 4-shot In-context Learning configuration. Four instances are randomly selected from the remaining dataset to provide context. We use extract string match to measure the output from LLMs and set the sampling upper bound times to  $10^5$ .

Task Name	Example
Dates	Input: 2015-10-22 Target: <u>!10!22!2015!</u>
Dates with unnatural form	Input: !08!24!1984! Target: <u>1984-08-24</u>
Identity	Input: a, b, c, d, e Target: <u>a, b, c, d, e</u>
Reverse Natural Content	Input: r, o, o, m, s Target: <u>s, m, o, o, r</u>

Table 7: Example Tasks in Unnatural In-context Learning Tasks

#### D.5 REMOVING DISTRACTING FACTOR IS IMPORTANT WHEN MEASURING TINY PERFORMANCE.

👉 We notice that removing the distracting factor is important when measuring the minor performance gain during scaling. The distracting factor means that a test instance is drastically different from the other test instance in terms of required abilities or evaluation bias. Note that we select the distracting factor based on the observation of test instances, which does not lead to information leakage when predicting the 2.4B model.

For Emoji Movie, some of the movie names are common words, enabling even a modestly sized model to “guess” them correctly based on our assessment criteria: the determination of model correctness is contingent upon the presence of movie names within the model’s output. Figure 8 shows that there is no significant association in the pass rates between models of varied scales. In other



words, the scaling law does not have much of an impact on model performance for these problems. Consequently, it becomes essential to exclude such distracting factors from consideration. We remove the movie names that are common words identified by the popular toolkit NLTK<sup>3</sup>.

For Date Understanding, we omit the following instance shown in Table 8. These instances only require the model to extract the answer from the context and don't require reasoning about the date.

In GPT-4 report (OpenAI, 2023), they split the HumanEval dataset into separate bins with different difficulties and conducted scaling prediction for each bin, thus removing the distraction of easy examples to hard examples.

Example
Today's meeting is rescheduled to 11 am tomorrow, 10/16/1924. What is the date tomorrow in MM/DD/YYYY?
Yesterday was 12/31/1929. Today could not be 12/32/1929 because December has only 31 days. What is the date yesterday in MM/DD/YYYY?
Today is 9/7. Jane is watching NFL 2003. What is the date today in MM/DD/YYYY?

Table 8: Distracting instances in Date Understanding Tasks.

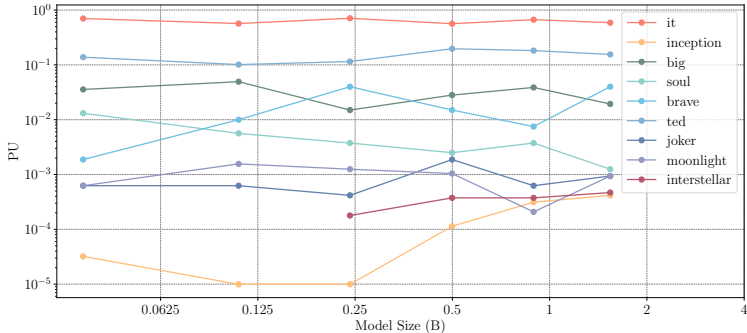


Figure 8: Large and small models have similar PU on these instances (mainly due to randomly sample from the vocabulary space), which creates distracting factors in our experiments.

## E ADDITIONAL EXPERIMENTAL RESULTS

In this section, we display some additional experimental results, including the additional fit curve of dataset level of PASSUNTIL, and the methods of utilizing test loss to assist the instance-level PASSUNTIL estimates.

### E.1 ADDITIONAL DATASET LEVEL PASSUNTIL RESULT.

The performances of series 2 models on HumanEval are represented in Figure 9. This prediction is less accurate compared to series 1. However, with instance level PASSUNTIL, the prediction precision improves.

### E.2 ESTIMATING PASSUNTIL FROM TEST LOSS

👉 As shown in Figure 10, we propose leveraging test loss on ground truth answers to assist the prediction for “hard samples”. For model series 1 and HumanEval task, the linear relationship is found to be  $PU \sim 0.22L$ . For model series 2 and HumanEval task, the linear relationship is found to be  $PU \sim 0.23L$ . For model series 2 and Date Understanding task, the linear relationship is found to be  $PU \sim 0.96L$ . And for model series 2 and Emoji Movie task, the linear relationship is found to be  $PU \sim 0.43L$ .

<sup>3</sup><https://www.nltk.org/>

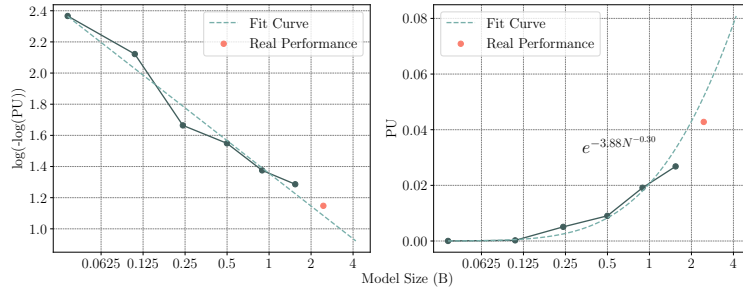


Figure 9: Additional figure on Test Loss Assisted PASSUNTIL Estimate.

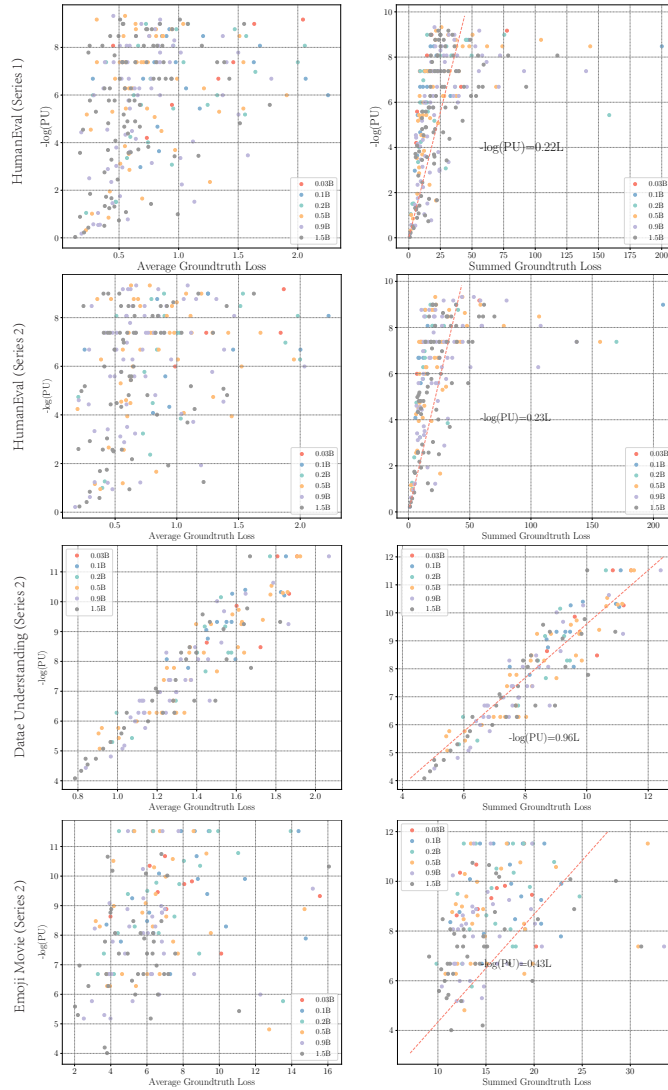


Figure 10: Additional figure on the relation between test loss and PASSUNTIL.

## E.3 MORE RESULT OF THE UNNATURAL IN-CONTEXT LEARNING TASKS

👉 We provide the scaling curves on the other two sub-tasks of the Unnatural In-context Learning tasks in Figure 11. We can see that the scaling curves exhibit a concave pattern between  $\log(\log(-F(N)))$  and  $\log N$ .

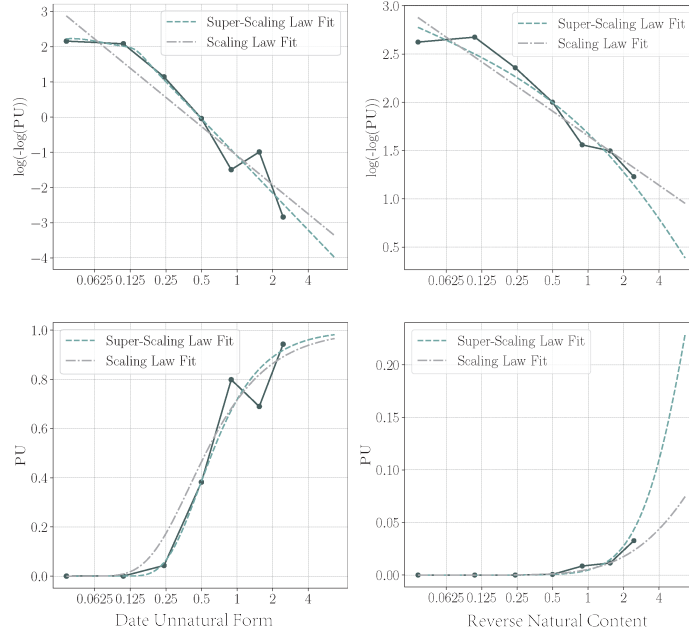


Figure 11: Additional figure on unnatural in-context learning. The grey line shows the scaling law fit, while the green line shows the super-scaling law fit.

## E.4 RESULT OF INDIVIDUAL PASSUNTIL ON MORE SAMPLES

👉 Figure 12 shows more instances of individual PASSUNTIL scaling curves of model series 1 on Humaneval task.

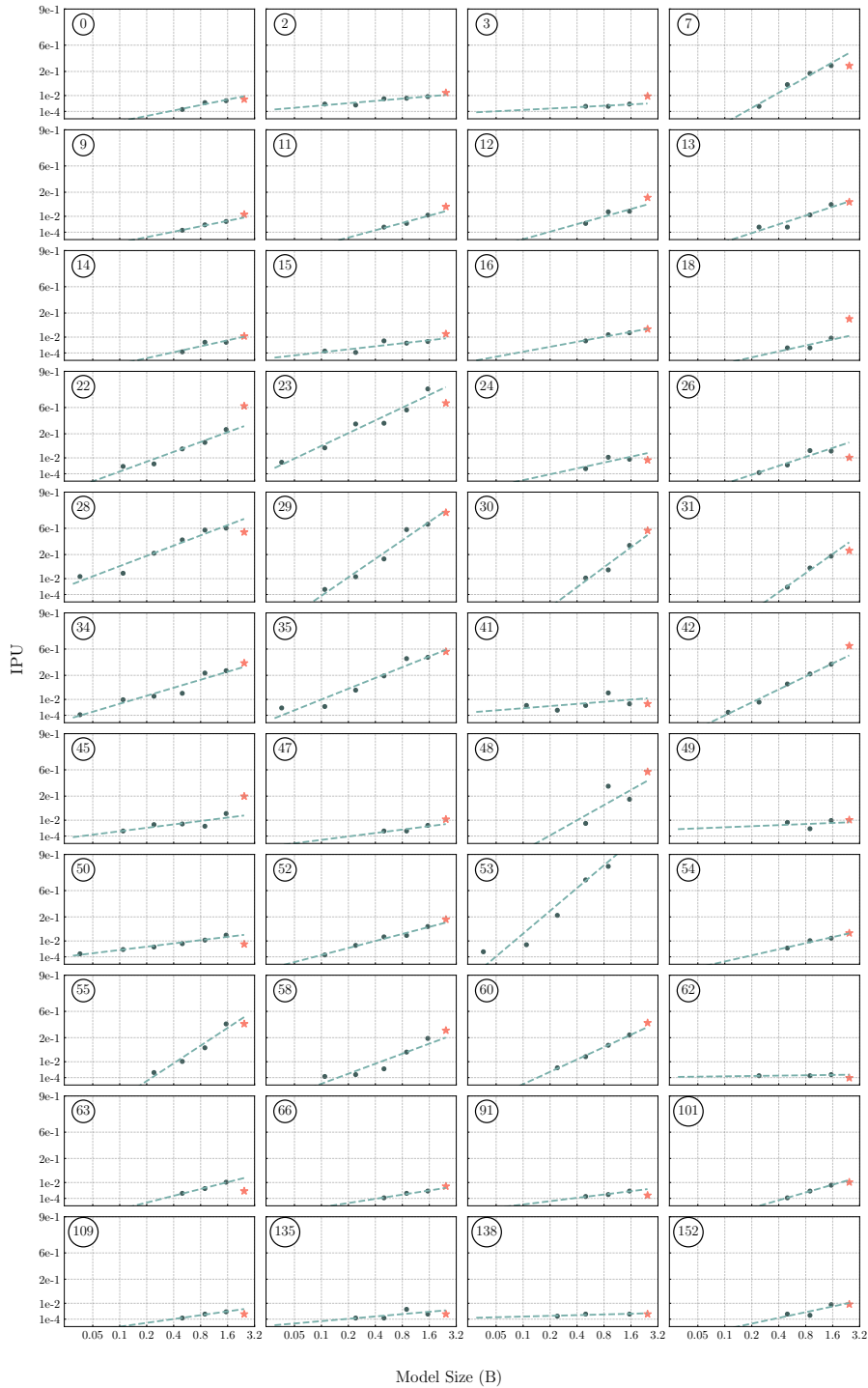


Figure 12: Result of instance-level scaling law fit. The label on the left upper corner of each subplot denotes the index of the sample in the test set<sup>4</sup>.

<sup>4</sup><https://github.com/openai/human-eval/tree/master/data>